

Asteroid models from combined sparse and dense photometric data

J. Āurech¹, M. Kaasalainen², B. D. Warner³, M. Fauerbach⁴, S. A. Marks⁴, S. Fauvaud^{5,6}, M. Fauvaud^{5,6}, J.-M. Vugnon⁶, F. Pilcher⁷, L. Bernasconi⁸, and R. Behrend⁹

¹ Astronomical Institute, Charles University in Prague V Holeřovičkách 2, 18000 Prague, Czech Republic
e-mail: durech@sirrah.troja.mff.cuni.cz

² Department of Mathematics and Statistics, Rolf Nevanlinna Institute, P.O.Box 68, FI-00014, University of Helsinki, Finland

³ Palmer Divide Observatory, 17995 Bakers Farm Rd., Colorado Springs, CO 80908, USA

⁴ Florida Gulf Coast University, 10501 FGCU Boulevard South, Fort Myers, FL 33965, USA

⁵ Observatoire du Bois de Bardou, F-16110 Taponnat, France

⁶ Association T60, 14, avenue Edouard Belin, F-31400 Toulouse, France

⁷ 4438 Organ Mesa Loop, Las Cruces, NM 88011, USA

⁸ Observatoire des Engarouines, 84570 Mallemort-du-Comtat, France

⁹ Geneva Observatory, CH-1290 Sauverny, Switzerland

Received ???; accepted ???

ABSTRACT

Aims. Shape and spin state are basic physical characteristics of an asteroid. They can be derived from disc-integrated photometry by the lightcurve inversion method. Increasing the number of asteroids with known basic physical properties is necessary to better understand the nature of individual objects as well as for studies of the whole asteroid population.

Methods. We use the lightcurve inversion method to obtain rotation parameters and coarse shape models of selected asteroids. We combine sparse photometric data from the US Naval Observatory with ordinary lightcurves from the Uppsala Asteroid Photometric Catalogue and the Palmer Divide Observatory archive, and show that such combined data sets are in many cases sufficient to derive a model even if neither sparse photometry nor lightcurves can be used alone. Our approach is tested on multiple-apparition lightcurve inversion models and we show that the method produces consistent results.

Results. We present new shape models and spin parameters for 24 asteroids. The shape models are only coarse but describe the global shape characteristics well. The typical error in the pole direction is $\sim 10\text{--}20^\circ$. For a further 18 asteroids, inversion led to a unique determination of the rotation period but the pole direction was not well constrained. In these cases we give only an estimate of the ecliptic latitude of the pole.

Key words. minor planets, asteroids – photometry – models

1. Introduction

The lightcurve inversion method is a powerful tool to derive basic physical properties of asteroids (rotation periods, spin axis orientations, and shapes) from their disc-integrated lightcurves (Kaasalainen & Torppa 2001; Kaasalainen et al. 2001, 2002a). As has been proven by space probes, laboratory models, and adaptive optics images (Kaasalainen et al. 2001, 2005; Marchis et al. 2006), models derived by this method are good approximations of the real shapes of asteroids. In the standard approach, the lightcurve inversion method is applied to a set of typically tens of lightcurves observed during at least three or four apparitions – only then can the spin state and the corresponding shape be derived uniquely. Kaasalainen (2004)

showed that to derive a unique physical model it is not necessary to have dense lightcurves – i.e., brightness measurements that densely sample brightness variations during one revolution. Lightcurve inversion can also be used on so-called ‘sparse data’ that only sparsely sample brightness variations. Typically, sparse data consist of at most a few measurements per night. A set of more than about one hundred calibrated measurements sparse in time is fully sufficient for modelling as long as the photometric accuracy of the data is better than $\sim 5\%$ (Āurech et al. 2005, 2007). Sparse data that will be available from all-sky surveys such as Pan-STARRS, LSST or Gaia are extremely time-efficient in obtaining new asteroid models compared to the standard approach of observing individual objects. However, accurate sparse data are not yet available, and all asteroid models based on photometry were derived by inversion

of standard dense lightcurves (e.g., Kaasalainen et al. 2002b, 2004; Torppa et al. 2003).

The main challenge to be solved when inverting sparse data is the correct determination of the rotation period. Because there is no direct information about the rotation period in the data, the correct value has to be found by scanning the whole interval of possible values and looking for the best fit. This is a time consuming process that yields a unique period solution only if there are enough data points (more than about a hundred) and if the data photometric accuracy is better than about $\sim 5\%$. If these conditions are not fulfilled, there is usually more than one period with the same fit to the data (for more details see Ďurech et al. 2005, 2007). On the other hand, just one ordinary dense lightcurve usually defines the possible range of the rotation period well. As has been shown by Kaasalainen & Ďurech (2007), noisy sparse data can be combined with a few ordinary lightcurves and such combined data sets give in many cases a unique solution. When combining sparse data with dense lightcurves, inversion leads to a unique solution for the period even if sparse data are noisy and the number of dense lightcurves is small.

In this paper we present new asteroid models derived from combined data sets. We used sparse data from the US Naval Observatory, Flagstaff (USNO) and dense lightcurves from the Uppsala Asteroid Photometric Catalogue (UAPC, Lagerkvist et al. 2001) and from the archive of the Palmer Divide Observatory (PDO).

We also present the results of various tests that estimate the errors in pole directions and show that our results are reliable.

2. Combined data

As stated above, combining sparse and dense photometry can yield a unique model even in cases when neither sparse data nor lightcurves would be sufficient for modelling alone. Sparse data typically cover more apparitions carrying thus information about brightness variations for different geometries. Dense lightcurves, on the other hand, well define the rotation period and enable us to narrow down the search interval.

2.1. Standard lightcurves

Most of the photometric lightcurves we used were archived in UAPC. Apart from this source, we also used the database of lightcurves of more than 200 asteroids observed at the Palmer Divide Observatory.¹ We also included new observations of (34) Circe and (416) Vaticana. Circe was observed by F. Pilcher (Las Cruces, New Mexico, 35-cm telescope) in 2007 and by M. Fauerbach and S. A. Marks (Egan Observatory, Florida, 40-cm telescope) in 2007/2008. Vaticana was observed in 2006/2007 by M. Fauerbach (Egan Observatory, Florida, 40-cm telescope) and by S. Fauvaud, J.-M. Vugnon, and M. Fauvaud (Pic du Midi Observatory, France, 60-cm telescope).

¹ <http://www.minorplanetobserver.com/PDO/PDOLightcurves.htm>

Table 1. Test asteroids. For each asteroid, the table gives the Δ_{\max} difference between the pole direction of the model derived from the full set of lightcurves and that derived from N_{lc} lightcurves and N_{sp} sparse points. In most cases, there are two values of Δ_{\max} for one N_{lc} column. This corresponds to two models with $\lambda \pm 180^\circ$ ambiguity in the pole direction.

| Asteroid | N_{sp} | Δ_{\max} (deg) | | | | | | | |
|----------------|----------|-----------------------|--------------|--------------|--------------|----|----|-----|-----|
| | | $N_{lc} = 6$ | $N_{lc} = 4$ | $N_{lc} = 2$ | $N_{lc} = 1$ | | | | |
| 3 Juno | 171 | | 15 | | | | | | |
| 15 Eunomia | 147 | 10 | | | | | | | |
| 32 Pomona | 128 | | 25 | | 13 | | | | |
| 39 Laetitia | 181 | | | 15 | | | | | |
| 43 Ariadne | 114 | 2 | | | | | | | |
| 44 Nysa | 170 | 11 | | | | | | | |
| 63 Ausonia | 137 | 4 | 3 | 5 | 7 | 9 | 8 | 13 | 12 |
| 107 Camilla | 116 | 9 | 2 | 2 | 5 | 2 | 9 | | |
| 125 Liberatrix | 105 | | | | | | | 146 | 145 |
| 130 Elektra | 113 | 4 | | 12 | | | | | 7 |
| 158 Koronis | 135 | 26 | 23 | | | | | | |
| 192 Nausikaa | 174 | 75 | | | | | | | |
| 201 Penelope | 115 | 6 | 3 | | | | | | |
| 277 Elvira | 93 | 7 | | | | 8 | 5 | | |
| 283 Emma | 96 | 4 | 6 | 6 | 6 | 50 | 8 | 3 | 6 |
| 306 Unitas | 130 | 2 | 3 | 5 | 4 | 6 | 5 | 7 | 8 |
| 382 Dodona | 121 | 8 | | 21 | 8 | 20 | 23 | 21 | 21 |
| 532 Herculina | 135 | 15 | | | | | | | |
| 584 Semiramis | 97 | 18 | | 20 | | 15 | | | |
| 665 Sabine | 118 | 11 | | 13 | | | | 16 | |
| 675 Ludmilla | 159 | 13 | 10 | 16 | 19 | 20 | 19 | 21 | 23 |
| 1627 Ivar | 68 | | | 18 | | | | | |

2.2. Sparse data

Sparse photometric data accurate enough to provide a unique solution of the inverse problem are not yet available. However, to obtain new asteroid models we need not wait for them – we can use already available less accurate sparse photometry and combine it with dense lightcurves. A huge amount of sparse photometry is provided each night by many observatories that carry out astrometric observations. Unfortunately, as these measurements are not intended for further photometric analysis, their quality is usually very poor from the photometric point of view. The only exceptions (as far as we know) are measurements made at the USNO. We estimated the typical error of these data to be ~ 0.08 – 0.1 mag. The database of astrometric measurements from the USNO is available at the Asteroid Dynamic Site². The data are available for the first 2000 numbered asteroids; they cover about five years and typically consist of 50–200 individual measurements.

3. Tests

Because our aim was to derive asteroid models based on noisy sparse data and a small number of dense lightcurves, we carried out various tests to determine how accurate and reliable the obtained results were.

² <http://hamilton.dm.unipi.it>

For our tests, we used the Database of Asteroid Models from Inversion Techniques (DAMIT)³ now containing about 80 models derived from dense lightcurves. From DAMIT, we selected 60 asteroids that had enough sparse USNO data (more than 30 points). From the full set of dense photometry for each asteroid, we randomly selected individual lightcurves and combined them with the sparse data to create test data sets. For each asteroid, we created twelve different test data sets: one set with six lightcurves ($N_{lc} = 6$) from three apparitions, two sets with four lightcurves ($N_{lc} = 4$) from two apparitions, three sets with two lightcurves ($N_{lc} = 2$) from one apparition, and six individual lightcurves ($N_{lc} = 1$). Each data set also contained sparse USNO data. We then processed the test data sets the same way as the real data using the lightcurve inversion method (Kaasalainen 2004; Ďurech et al. 2005, 2007). The inversion algorithm derives a spin/shape model that minimizes the difference between observed and computed brightness. The minimization process can use dense and sparse data and we decided to weight the sparse data one third of the dense data. We used information about rotation periods and reliability codes listed in the Minor Planet Lightcurve Parameters database.⁴ All asteroids from DAMIT have reliability codes 3 or 4. For each asteroid, we scanned an interval of periods centered at the reported period P with a width of $\pm 1\%$ and $\pm 3\%$ of P for reliability codes 4 and 3, respectively.⁵

As expected, in most cases the limited amount of data was not sufficient to provide us with a unique solution – out of the 60 asteroids and 12 tests for each asteroids there were only 22 asteroids that had at least one unique solution. A *unique solution* was defined as follows: the best period had at least 10% lower χ^2 than all other periods from the scanned interval and, for this period, there was only one pole solution with at least 10% lower χ^2 than the others (with a possible mirror solution for $\lambda \pm 180^\circ$).

We compared the obtained results with the models from DAMIT based on full lightcurve sets – the DAMIT models were taken as established. Results listed in Table 1 report the maximum difference Δ_{max} (in degrees) between the pole solution for the corresponding test data set with N_{lc} lightcurves and the original DAMIT solution based on a full set. We do not report the difference in periods, since it was always within the expected error (the two exceptions (125) Liberatrix and (192) Nausikaa are discussed below). If there were more solutions for different test data sets with the same N_{lc} , we chose always the largest difference between the true model and the derived one. Thus Table 1 reports the worst-case scenario results. From the values of Δ_{max} , we can estimate the reliability of pole/period

Table 2. Difference in the pole ecliptic latitude β for multiple-pole solutions with a unique determination of the period but unconstrained value of the pole longitude λ and the variation in β less than 50° . For each asteroid, the table gives the $\Delta\beta_{max}$ difference between the pole latitude of the model derived from the full set of lightcurves and the mean value of β for non-unique models derived from N_{lc} lightcurves and N_{sp} sparse points.

| Asteroid | N_{sp} | $\Delta\beta_{max}$ [deg] | | | |
|----------------|----------|---------------------------|--------------|--------------|--------------|
| | | $N_{lc} = 6$ | $N_{lc} = 4$ | $N_{lc} = 2$ | $N_{lc} = 1$ |
| 3 Juno | 171 | 29 | | | |
| 15 Eunomia | 147 | | 7 | 7 | 4 |
| 19 Fortuna | 213 | 4 | | | |
| 20 Massalia | 143 | | 0 | | |
| 32 Pomona | 128 | 21 | 18 | 18 | 20 |
| 39 Laetitia | 181 | | 28 | | |
| 44 Nysa | 170 | | 11 | | 0 |
| 107 Camilla | 116 | | 4 | 4 | 3 |
| 125 Liberatrix | 105 | | 21 | 21 | |
| 129 Antigone | 149 | 3 | 1 | 1 | 1 |
| 135 Hertha | 102 | 21 | | 0 | |
| 158 Koronis | 135 | | 4 | 4 | 5 |
| 192 Nausikaa | 174 | | 64 | | |
| 277 Elvira | 93 | | 14 | | |
| 306 Unitas | 130 | | | 0 | 19 |
| 382 Dodona | 121 | | | | 0 |
| 584 Semiramis | 97 | | 22 | 22 | |
| 665 Sabine | 118 | | | 0 | 24 |
| 1223 Neckar | 96 | | | | 0 |
| 1627 Ivar | 68 | | | | 0 |

solutions based on combined data. If no unique solution was found for any test data set with a given N_{lc} , we had nothing to compare and the value of Δ_{max} for the corresponding N_{lc} is missing. If there are two values of Δ_{max} in one N_{lc} column, they correspond to two established models ($\lambda \pm 180^\circ$ ambiguity) in DAMIT.

Apart from the asteroids Liberatrix, Nausikaa, and Emma that are discussed below, we obtained a correct solution for the period and a pole for all test asteroids. The pole difference was never greater than $\sim 25^\circ$. This justifies the use of combined data sets for lightcurve inversion and gives credibility to new asteroid models derived in Sect. 4.

(125) Liberatrix This case revealed the limits of combined data sets. Although the sparse data consisted of more than one hundred points, in one test case these data combined with only one dense lightcurve led to an incorrect period, thus to an incorrect pole direction and an incorrect shape model. The correct rotation period, 3.9682 hr, gave the second best χ^2 that was $\sim 10\%$ higher than the lowest χ^2 for the period of 3.9491 hr. There were no unique period solutions for the other eleven test data sets.

(192) Nausikaa This asteroid gave a large difference between the solution derived from the combined data set (six lightcurves from three apparitions and sparse data) and the original solution by Kaasalainen et al. (2002b). However, the new analysis

³ <http://astro.troja.mff.cuni.cz/projects/asteroids3D>

⁴ <http://cfa-www.harvard.edu/iau/lists/LightcurveDat.html>

⁵ The meaning of reliability codes is as follows (according to the Minor Planet Lightcurve Parameters database): Code 2 – Result based on less than full coverage, so that the period may be wrong by about 30%. Also used to indicate cases where an ambiguity exists as to the number of extrema between lightcurves. Hence the result may be wrong by an integer ratio. Code 3 – Secure result with no ambiguity, full lightcurve coverage. Code 4 – In addition to full coverage, denotes that a pole position is reported.

of all available lightcurves showed that the published result is only one of further possible solutions. More observations are needed to derive a unique model.

(283) Emma One solution based on sparse data and two lightcurves from one apparition gave a pole solution as far as 50° from the correct one. This again shows that data from one apparition with only one or two lightcurves may lead to an incorrect solution. However, all other combinations of test data led to solutions that were very close (difference in pole directions $< 10^\circ$) to the true one.

(675) Ludmilla The model of asteroid Ludmilla published by Torppa et al. (2003) was inconsistent with new observations carried out by Bernasconi⁶. We derived a new model (available now in DAMIT) that was fully consistent with all available lightcurves and also with sparse data. Values of Δ_{\max} in Table 1 and Table 3 are based on the new model with the spin axis direction (in ecliptic coordinates) $\lambda = 49^\circ$, $\beta = 74^\circ$ (mirror solution $\lambda = 196^\circ$, $\beta = 49^\circ$) and the sidereal rotation period $P = 7.715486$ h.

We emphasize that DAMIT contains updated versions of asteroid models; several models published in the papers cited above have changed, some of them significantly. This is mostly due to updated data sets, but we note that software errors and/or too narrow ranges for the initial period have affected the quality of some models, whose corrected versions now appear in DAMIT. Thus, while citing the original paper in which the model for a given asteroid appears, one should always download the updated model information from DAMIT and not use the obsolete information given in the paper. Shortly, we will submit an online paper describing the database.

3.1. Determination of the pole ecliptic latitude β

Even if the rotation period of an asteroid can be determined uniquely, there can be more than one independent pole solution for this period that fit all observed data well. We have noticed that often in such cases, there are more possible pole solutions with very different values of the ecliptic longitude λ but very similar values of the ecliptic latitude β – thus we can take β as a well determined parameter.⁷ Although we cannot determine the ecliptic longitude λ and the corresponding shape model, the ecliptic latitude β of the spin axis is an important physical parameter. For asteroids with small or moderate inclinations, β directly gives the obliquity – the angle between the rotation axis and the normal to the orbital plane.

Using the same test data sets and inversion procedure as in the previous test, we selected such solutions that had no unique shape and pole, but a unique period and poles with β values within an interval of 50° . Table 2 lists results for 20 such mul-

Table 3. The same test as in Table 1 but the number of sparse data points was reduced to $N_{\text{sp}} = 50$.

| Asteroid | Δ_{\max} (deg) | | |
|---------------|-----------------------|---------------------|---------------------|
| | $N_{\text{lc}} = 6$ | $N_{\text{lc}} = 4$ | $N_{\text{lc}} = 2$ |
| 2 Pallas | | | 95 98 |
| 15 Eunomia | | 19 | 40 |
| 21 Lutetia | | | 41 37 |
| 39 Laetitia | 16 | 12 | 28 |
| 43 Ariadne | 2 | 1 | |
| 44 Nysa | 9 | | 104 |
| 63 Ausonia | | 3 2 | 7 9 |
| 107 Camilla | 1 4 | 9 7 | 3 13 |
| 130 Elektra | | 7 | 2 |
| 201 Penelope | 5 8 | | |
| 277 Elvira | 11 10 | 22 11 | 8 2 |
| 283 Emma | 3 3 | 9 6 | |
| 306 Unitas | | 4 2 | |
| 311 Claudia | 22 28 | | 32 37 |
| 382 Dodona | 12 2 | 27 14 | 20 19 |
| 532 Herculina | 14 | | 7 |
| 534 Nassovia | | 20 18 | |
| 584 Semiramis | 9 | | |
| 624 Hektor | 7 | | |
| 665 Sabine | | | 25 |
| 675 Ludmilla | 10 15 | 8 17 | 87 96 |
| 1223 Neckar | 11 5 | | |
| 1627 Ivar | | 18 | 19 |

iple pole solutions and reports the maximum difference $\Delta\beta_{\max}$ between the mean value of β for models based on our test data set and β of the original model. This difference was so small in some cases that $\Delta\beta_{\max}$ was zero after truncation. Again, this is the worst-case scenario, which means that we report the largest values if there are more solutions for different test data sets with the same N_{lc} . If there were more solutions for the period, or the derived poles for a unique period were different by more than 50° in β , the value of $\Delta\beta_{\max}$ is missing. In some cases (for example (32) Pomona or (107) Camilla), there are values of Δ_{\max} in Table 1 and $\Delta\beta_{\max}$ in Table 2 for the same N_{lc} column. This means that the values of Δ_{\max} and $\Delta\beta_{\max}$ were derived for different data sets with the same N_{lc} . One test yielded a unique solution and was listed in Table 1, while the other fulfilled the conditions mentioned above and was listed in Table 2. The only asteroid showing a large discrepancy between β values of the published and derived model is again Nausikaa. All other asteroids have differences in β lower than $\sim 30^\circ$, which is enough for a rough determination of the obliquity.

3.2. Limited amount of sparse data

The number of sparse data points for asteroids from our tests was usually more than one hundred (see Table 1). On the other hand, some sparse data used to derive new models in Sect. 4 consisted of fewer than one hundred points (see Table 5). In order to test what happens if we use less sparse data and to find out how reliable the derived models are, we reduced the amount of sparse data. We used the same test data sets as in Sect. 3 but instead of using all available sparse data we ran-

⁶ <http://obswww.unige.ch/~behrend/page2cou.html#000675>

⁷ The well-known $\lambda \pm 180^\circ$ ambiguity in the spin axis direction is inevitable for disk-integrated measurements in the plane of the ecliptic (Kaasalainen & Lamberg 2006; Kaasalainen & Ďurech 2007).

Table 4. The same test as in Table 2 but the number of sparse data points was reduced to $N_{\text{sp}} = 50$.

| Asteroid | $\Delta\beta_{\text{max}}$ (deg) | | |
|---------------|----------------------------------|---------------------|---------------------|
| | $N_{\text{lc}} = 6$ | $N_{\text{lc}} = 4$ | $N_{\text{lc}} = 2$ |
| 15 Eunomia | 6 | | 3 |
| 23 Thalia | | | 48 |
| 32 Pomona | | | 33 |
| 44 Nysa | | | 97 |
| 129 Antigone | | 7 | |
| 158 Koronis | 6 | | |
| 277 Elvira | | | 14 |
| 311 Claudia | | 4 | |
| 382 Dodona | | | 22 |
| 511 Davida | | | 5 |
| 532 Herculina | | 24 | 17 |
| 584 Semiramis | | 22 | |
| 665 Sabine | 24 | 23 | 14 |

domly selected only 50 points. We applied the same inversion procedure and uniqueness conventions as when using the complete data. Results for full period/pole/shape models are listed in Table 3 and those for partial models with only P and β determination are listed in Table 4. Naturally, with less sparse data, the discrepancy between original DAMIT models and derived models is now greater. Results from Tables 3 and 4 show that if the number of sparse data points is low, it is necessary to have dense lightcurves from at least two apparitions ($N_{\text{lc}} = 4$) to derive a reliable model. For lightcurves from only one apparition ($N_{\text{lc}} = 2$), the inversion method gives incorrect results. However, the results derived from combined data with dense lightcurves from two or more apparitions are still in good agreement with the models based on full data sets.

For some asteroids (for example (2) Pallas or (21) Lutetia), we obtained formally unique solutions (according our definition) when using reduced amount of sparse data, whereas there was no unique solution for any test data set when using complete sparse data.

3.3. Tests – conclusions

The performed tests showed that if a typical combined data set (around one hundred sparse points observed over five years and a few lightcurves from two or more apparitions) leads to a unique solution of the inverse problem, then this solution is very close to the solution based on the full data set of dense lightcurves. The period is determined correctly within the expected error. The uncertainty in the pole direction is $20\text{--}25^\circ$ at most with a typical value $\sim 10\text{--}20^\circ$. Derived shape models are coarse and represent only basic characteristics of shape. As an example, there are three models of asteroid (130) Elektra in Fig. 1. The model derived from the full set of dense lightcurves (49 lightcurves from 8 apparitions) is compared with the model derived from the full sparse data (113 points) and one dense lightcurve and with the model derived from sparse data reduced to 50 points and four dense lightcurves from two apparitions. The sparse+dense models look rougher because their shapes are represented by spherical harmonics series, whereas

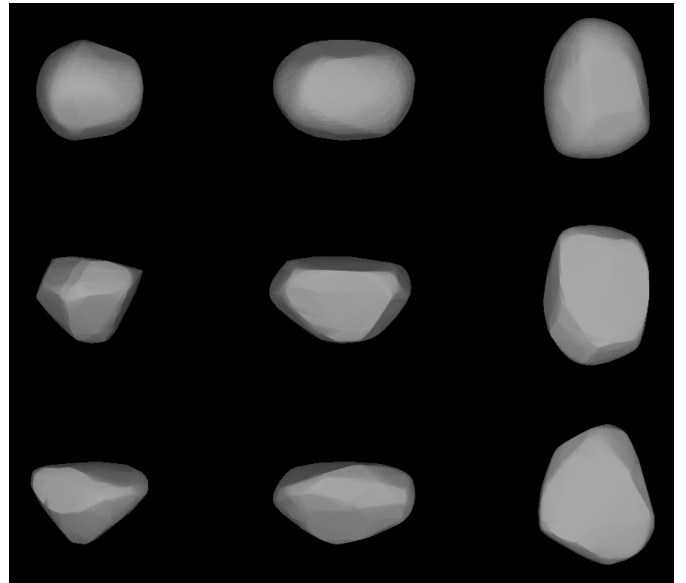


Fig. 1. Top: a convex shape model of (130) Elektra based on 49 standard lightcurves from 8 apparitions. Middle: a shape model based on sparse data (113 points) and one standard lightcurve. Bottom: a shape model based on reduced sparse data (50 points) and four standard lightcurves from two apparitions. Models are shown from the equator (left, center) and pole-on (right). The difference in pole directions between the full-set model and those derived using combined data is 7° in both cases.

the full-set model looks smoother because it has higher resolution and is represented directly by areas of surface facets (see Kaasalainen & Torppa 2001). Due to limited geometry and a small number of data points, sparse photometry usually does not allow us to reconstruct a higher-resolution model. However, the global shape features of all models are similar and the difference between pole directions of the full-set model and both sparse-data models is only 7° .

4. Results

We combined lightcurves from UAPC and PDO with sparse data from USNO, obtaining combined data sets for about 470 asteroids (350 from UAPC and 120 from PDO). We removed clear outliers from the sparse data and then applied the lightcurve inversion method to these combined data sets as described in Kaasalainen (2004); Ďurech et al. (2005, 2007). Because we had a priori information about the rotation periods of individual asteroids (taken from the Minor Planet Lightcurve Database) we could restrict the period search interval to a relatively narrow range of 1, 3, and 10% around the reported value of period for reliability codes 4, 3, and 2, respectively.⁸ For most asteroids in our sample, the data were insufficient to derive a unique model – usually there were more than one equally good solutions for the rotation period or there were multiple independent pole solutions for one period. We derived 24 models (listed in Table 5) that were unique according to the definition from Sect. 3: a unique solution gives at least 10% lower χ^2 than

⁸ The meaning of reliability codes is explained in the footnote in Sect. 3.

Table 5. Spin state solutions for models derived from combined data sets. For each asteroid, the table lists the ecliptic longitude λ_1 and latitude β_1 of the pole direction (with a possible mirror solution λ_2, β_2), the rotation period P , the number of sparse data points N_{sp} , the number of dense lightcurves N_{lc} observed during N_{app} apparitions, and a note on the source of dense lightcurves (UAPC – Uppsala Asteroid Photometric Catalogue, PDO – Palmer Divide Observatory).

| Asteroid | λ_1 [deg] | β_1 [deg] | λ_2 [deg] | β_2 [deg] | P [hours] | N_{sp} | N_{lc} | N_{app} | Note |
|------------------|----------------------|--------------------|----------------------|--------------------|--------------|-----------------|-----------------|------------------|-----------------|
| 5 Astraea | 126 | 40 | 310 | 44 | 16.80061 | 153 | 24 | 7 | UAPC |
| 17 Thetis | 55 | 10 | 236 | 20 | 12.26603 | 221 | 52 | 8 | UAPC |
| 30 Urania | 107 | 23 | 284 | 20 | 13.68717 | 106 | 11 | 3 | UAPC |
| 34 Circe | 94 | 35 | 275 | 51 | 12.17458 | 114 | 16 | 5 | UAPC + new obs. |
| 80 Sappho | 6 | -16 | 194 | -26 | 14.03087 | 125 | 12 | 4 | UAPC |
| 82 Alkmene | 164 | -34 | 351 | -39 | 13.00078 | 129 | 11 | 1 | UAPC |
| 132 Aethra | 337 | 70 | | | 5.168274 | 174 | 4 | 2 | UAPC |
| 146 Lucina | 139 | -14 | 305 | -41 | 18.55397 | 125 | 22 | 4 | UAPC |
| 152 Atala | 199 | 62 | 347 | 47 | 6.24472 | 101 | 2 | 1 | UAPC |
| 182 Elsa | 72 | -84 | 224 | -82 | 80.166 | 118 | 9 | 2 | UAPC |
| 184 Dejopeja | 14 | 51 | 196 | 50 | 6.441119 | 133 | 4 | 2 | UAPC |
| 278 Paulina | 123 | 45 | 311 | 28 | 6.49387 | 154 | 3 | 1 | UAPC |
| 360 Carlova | 129 | 65 | 350 | 55 | 6.189596 | 143 | 6 | 2 | UAPC |
| 416 Vaticana | 291 | 12 | | | 5.371597 | 131 | 24 | 2 | UAPC + new obs. |
| 484 Pittsburghia | 69 | 47 | | | 10.64976 | 100 | 2 | 1 | UAPC |
| 516 Amherstia | 80 | 53 | 253 | 22 | 7.48430 | 125 | 5 | 2 | UAPC |
| 614 Pia | 165 | 32 | 354 | 45 | 4.57870 | 86 | 2 | 1 | UAPC |
| 628 Christine | 24 | -61 | 209 | -34 | 16.17293 | 117 | 6 | 1 | PDO |
| 714 Ulula | 40 | -4 | 225 | -13 | 6.99838 | 156 | 4 | 1 | UAPC |
| 770 Bali | 68 | 44 | 256 | 40 | 5.81894 | 87 | 2 | 1 | UAPC |
| 849 Ara | 17 | -10 | 213 | -33 | 4.116391 | 133 | 5 | 1 | UAPC |
| 915 Cosette | 185 | 50 | 348 | 55 | 4.469741 | 88 | 1 | 1 | UAPC |
| 1012 Sarema | 51 | 64 | 254 | 53 | 10.30708 | 74 | 2 | 1 | UAPC |
| 1088 Mitaka | 115 | -46 | 278 | -72 | 3.035377 | 74 | 1 | 1 | UAPC |

Table 6. Partial spin state solutions for asteroids with an ambiguous pole solution. For each asteroid, the table lists the mean ecliptic latitude β of the pole direction and its dispersion Δ . The other parameters are the same as in Table 5.

| Asteroid | β [deg] | Δ [deg] | P [hours] | N_{sp} | N_{lc} | N_{app} | Note |
|-----------------|------------------|-------------------|--------------|-----------------|-----------------|------------------|------|
| 28 Bellona | -6 | 17 | 15.70785 | 130 | 8 | 3 | UAPC |
| 119 Althaea | -62 | 8 | 11.46512 | 102 | 4 | 2 | UAPC |
| 136 Austria | 63 | 21 | 11.49660 | 130 | 4 | 1 | UAPC |
| 312 Pierretta | -52 | 12 | 10.20768 | 118 | 4 | 1 | UAPC |
| 355 Gabriella | 69 | 7 | 4.82899 | 128 | 4 | 1 | UAPC |
| 390 Alma | -64 | 18 | 3.74116 | 109 | 2 | 1 | PDO |
| 394 Arduina | -71 | 16 | 16.6218 | 108 | 8 | 1 | UAPC |
| 540 Rosamunde | 57 | 9 | 9.34778 | 96 | 3 | 1 | UAPC |
| 544 Jetta | -66 | 19 | 7.74526 | 104 | 3 | 1 | PDO |
| 550 Senta | -64 | 18 | 20.5727 | 103 | 9 | 1 | UAPC |
| 636 Erika | -52 | 14 | 14.60755 | 135 | 6 | 1 | UAPC |
| 825 Tanina | 54 | 9 | 6.93981 | 114 | 2 | 1 | UAPC |
| 966 Muschi | -57 | 17 | 5.35531 | 111 | 3 | 1 | PDO |
| 1089 Tama | -21 | 20 | 16.4655 | 61 | 1 | 1 | UAPC |
| 1188 Gothlandia | -52 | 15 | 3.491820 | 98 | 2 | 1 | UAPC |
| 1207 Ostenia | -57 | 13 | 9.07129 | 87 | 2 | 1 | UAPC |
| 1270 Datura | 59 | 12 | 3.358100 | 79 | 2 | 1 | UAPC |
| 1514 Ricouxa | 71 | 16 | 10.42466 | 68 | 3 | 1 | UAPC |

all others outside the range of parameter errors. The weight of sparse data was one third of that of dense lightcurves. However, the models we present are not sensitive to the particular choice of weighting. The uncertainty in the rotation period depends on the length of observation interval and corresponds to the or-

der of the last decimal place of period P in Tables 5 and 6. The uncertainty in the pole direction depends on the number of lightcurves and sparse data points and, according to tests, is usually $\sim 10\text{--}20^\circ$.

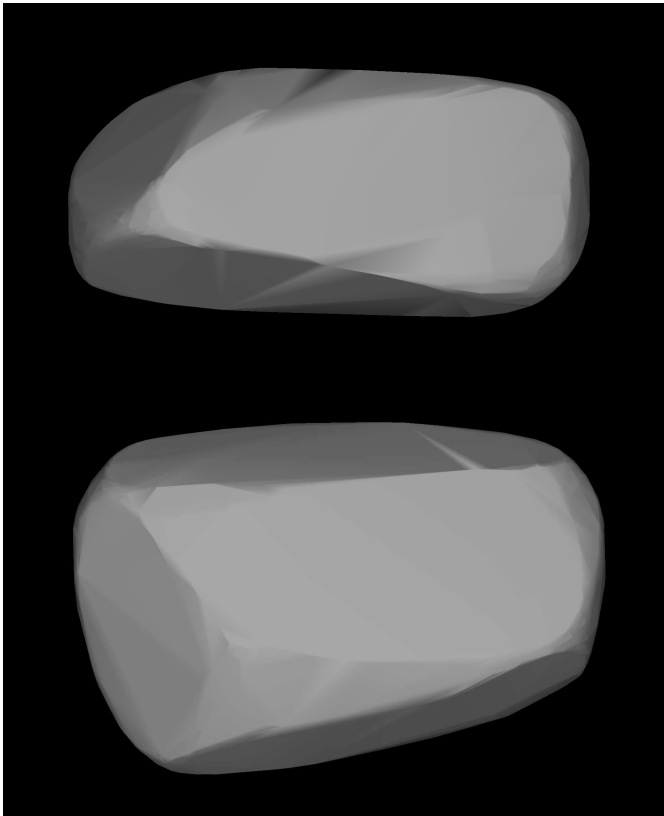


Fig. 2. A possible convex shape model of (1089) Tama shown from the equator (top) and pole-on (bottom). The flat surfaces indicate possible binarity. The model was derived from only 61 sparse data points and one dense lightcurve.

We also derived 18 partial models (listed in Table 6) with a uniquely determined rotation period and a rough estimation of the pole ecliptic latitude β . Each value of β given in Table 6 is a mean of the pole ecliptic latitudes for different models if their dispersion was not larger than 50° . The parameter Δ in Table 6 gives the estimated error of β , $\Delta = |\beta_{\max} - \beta_{\min}|/2$, where β_{\max} and β_{\min} are extremal values of β for individual solutions.

4.1. Selected objects

(184) Dejopeja A model of Dejopeja was recently derived by Marciniak et al. (2007). Their pole solutions ($18^\circ, +54^\circ$) and ($201^\circ, +52^\circ$) are only a few degrees away from our solutions based on only four lightcurves from two apparitions and 133 sparse data points.

(1089) Tama The binary nature of this asteroid was revealed by Behrend et al. (2004). We were not able to obtain a unique model. In Fig. 2, we present one possible solution with the pole direction ($181^\circ, -8^\circ$). Although the solution is derived from only one flat dense lightcurve and 61 sparse points, the shape model indicates that the asteroid could be a binary. In general, convex shape models cannot describe binary objects. However, flat shape models with rectangular pole-on silhouettes are typical results when inverting lightcurves of synchronous binaries (Ďurech & Kaasalainen 2003). According to Table 4, results

derived for Tama should be taken with care due to the small number of lightcurves and sparse points. However, because Tama's brightness variations have a large amplitude of ~ 1 mag (Behrend et al. 2006), the lightcurve signal is so strong that even a small number of noisy measurements yields a unique and robust solution for the rotation period.

5. Conclusions

After the theoretical work of Kaasalainen (2004) and simulations made by Ďurech et al. (2005, 2007), this paper is the first example of using real sparse data for asteroid modelling. The results we obtained clearly show that even noisy sparse data carry information about asteroid brightness variations caused by rotation and shape, and that they can be used as complementary data to ordinary lightcurves. Apart from asteroids (34) Circe and (416) Vaticana, all new models were derived just by ‘data mining’ of UAPC, PDO, and USNO catalogues. Although models derived from a limited number of dense lightcurves and noisy sparse data are not as accurate as standard models from multiple-apparition photometry, 24 new models significantly increase the number of asteroids with known spin states and shapes (DAMIT contains about 80 asteroid models). The 18 partial models with unknown λ but roughly estimated β can be used for statistical studies. All derived models are available through the DAMIT web page and will be updated when new observations are available. The source codes for lightcurve inversion software are also available on the DAMIT web page. We will describe the software packages in detail in a forthcoming paper.

In the near future, sparse photometric observations from sky surveys will drastically enlarge the number of asteroid models to 10^4 or even 10^5 , allowing us to obtain comprehensive maps of various asteroid populations. Dense lightcurves will be important in this study. In addition to constructing the subset of best-defined models from sky surveys, they facilitate quality and reliability checks for the photometric data and the modelling pipelines of the surveys. They also serve as follow-up data for objects labelled especially interesting in the sparse photometry pipelines. Thus, dedicated dense lightcurve observation campaigns for a large number of objects will be more important than ever.

Acknowledgements. The work of JĎ was supported by the grant GACR 205/07/P070 of the Czech grant agency and by the Research Program MSM0021620860 of the Ministry of education. The work of MK was supported by the Academy of Finland. Funding for BDW was provided by NASA grant NNG06GI32G and by the National Science Foundation grant AST-0607505 and a Shoemaker NEO grant from the Planetary Society.

References

- Behrend, R., Bernasconi, L., Roy, R., et al. 2006, A&A, 446, 1177
- Behrend, R., Roy, R., Rinner, C., et al. 2004, IAU Circ., 8265, 2
- Ďurech, J. & Kaasalainen, M. 2003, A&A, 404, 709

- Ďurech, J., Grav, T., Jedicke, R., Kaasalainen, M., & Denneau, L. 2005, *Earth, Moon, and Planets*, 97, 179
- Ďurech, J., Scheirich, P., Kaasalainen, M., et al. 2007, in *Near Earth Objects, our Celestial Neighbors: Opportunity and Risk*, ed. A. Milani, G. B. Valsecchi, & D. Vokrouhlický (Cambridge: Cambridge University Press), 191
- Kaasalainen, M. & Torppa, J. 2001, *Icarus*, 153, 24
- Kaasalainen, M., Torppa, J., & Muinonen, K. 2001, *Icarus*, 153, 37
- Kaasalainen, M., Mottola, S., & Fulchignomi, M. 2002a, in *Asteroids III*, ed. W. F. Bottke, A. Cellino, P. Paolicchi, & R. P. Binzel (Tucson: University of Arizona Press), 139–150
- Kaasalainen, M., Torppa, J., & Piironen, J. 2002b, *Icarus*, 159, 369
- Kaasalainen, M. 2004, *A&A*, 422, L39
- Kaasalainen, M., Pravec, P., Krugly, Y. N., et al. 2004, *Icarus*, 167, 178
- Kaasalainen, S., Kaasalainen, M., & Piironen, J. 2005, *A&A*, 440, 1177
- Kaasalainen, M. & Lamberg, L. 2006, *Inverse Problems*, 22, 749
- Kaasalainen, M. & Ďurech, J. 2007, in *Near Earth Objects, our Celestial Neighbors: Opportunity and Risk*, ed. A. Milani, G. B. Valsecchi, & D. Vokrouhlický (Cambridge: Cambridge University Press), 151
- Lagerkvist, C.-I., Piironen, J., & Erikson, A. 2001, *Asteroid photometric catalogue, fifth update* (Uppsala Astronomical Observatory)
- Marchis, F., Kaasalainen, M., Hom, E. F. Y., et al. 2006, *Icarus*, 185, 39
- Marciniak, A., Michałowski, T., Kaasalainen, M., et al. 2007, *A&A*, 473, 633
- Torppa, J., Kaasalainen, M., Michałowski, T., et al. 2003, *Icarus*, 164, 346